INDONESIAN JOURNAL ON GEOSCIENCE
Geological Agency
Ministry of Energy and Mineral Resources

Journal homepage: http://ijog.geologi.esdm.go.id
ISSN 2355-9314, e-ISSN 2355-9306

Tholeiitic Basalt in Banyumas Basin (Kebasen, Central Java): The Evidence of Sedimentary Recycling Input and the Contribution of Oceanic Slab on Fore-arc Active Continental Margin (ACM) Magmatism

[1]Fadlin, [2]Shaban Godang, [3]Nita Ariyanti, [4]Wildan Nur Hamzah, and [1]Maulana Rizki Aditama

[1]Geological Engineering, Jenderal Soedirman University (UNSOED), Purwokerto, Indonesia
[2]Independent Geochemist, Geochemistry Tectonic Modelling and REE Researcher, Jakarta, Indonesia
[3]Geophysical Engineering, Sepuluh November Institute of Technology (ITS), Surabaya, Indonesia
[4]Geological Engineering, Bandung Institute of Technology (ITB), Bandung, Indonesia

Corresponding author: fadlin@unsoed.ac.id
Manuscript received: May, 18, 2018; revised: July, 15, 2019;
approved: September, 8, 2020; available online: July, 6, 2021

Abstract - The study of tholeiitic basalt is a general-classic study from geotectonic MORB, ocean island (OIB), continental rift, volcanic-arcs {IAB or Active Continental Margin (ACM)}. However, the geotectonic study of the tholeiitic volcanic-arcs is still unclear at the moment. In general, the arc tholeiitic is directly pointed to an island-arc volcanic, and the result of google search engine defines no existence of tholeiitic geochemistry which is formed from continental-arc volcanic (ACM). The problem lies in the model of discrimination diagram which is not able to discriminate ACM from the island arc volcanic. The spider diagram shows relatively similar of patterns as well as in the use of the isotope 143Nd/144Nd versus 87Sr/86Sr. Tholeiitic Kebasen pillow lava exhibits a slightly hydrothermal alteration (propyilitic alteration) which consists of plagioclase (labradorite-bytownite), olivine, pyroxene (diopside), hornblende, volcanic glass and other secondary minerals (such as iddingsite, zeolite, carbonate, sericite and opaque minerals). The results of the interpretation using the overlay diagram of Mg# and FeO(t)/MgO, diagram Nb/La vs. La/Yb, the overlaid diagram between the diagram of Zr/Y vs. Zr, newly developed diagram for sedimentary recycling (Th/Ce vs. SiO2) reveal the Kebasen lava is a differentiated tholeiitic rock with relatively low of Mg# (Mg# < 55) which is generated from geotectonic forearc ACM (Active Continental Margin) and involves the sedimentary recycling (Th/Ce > 0.1); furthermore, the trace element constituent is interpreted based upon the melting of oceanic slab (Zr/Y ~ 3). The magmatism of Kebasen lava is potentially formed at temperature of ~ 1240 ^{o}C and a pressure of ~ 1.7 GPa at the depth of ~ 56 Km.

Keywords: Kebasen, tholeiitic basalt, sedimentary recycling, oceanic slab melting,fore-arc ACM

How to cite this article:
Fadlin, Godang, S., Ariyanti, N., Hamzah, W.N., and Aditama, M.R., 2021. Tholeiitic Basalt in Banyumas Basin (Kebasen, Central Java): The Evidence of Sedimentary Recycling Input and the Contribution of Oceanic Slab on Fore-arc Active Continental Margin (ACM) Magmatism. *Indonesian Journal on Geoscience*, 8 (2), p.233-253. DOI: 10.17014/ijog.8.2.233-253

Introduction

Kebasen is a subregency which covers an area of 25 km^2. It is situated within the southern part of Banyumas Regency, Central Java Province, Indonesia, and located 19 km to the south of Purwokerto City (Figure 1). The studied area is part of the Banyumas Basin system which is included in the Southern Serayu Mountain physiography. The Southern Serayu Mountain

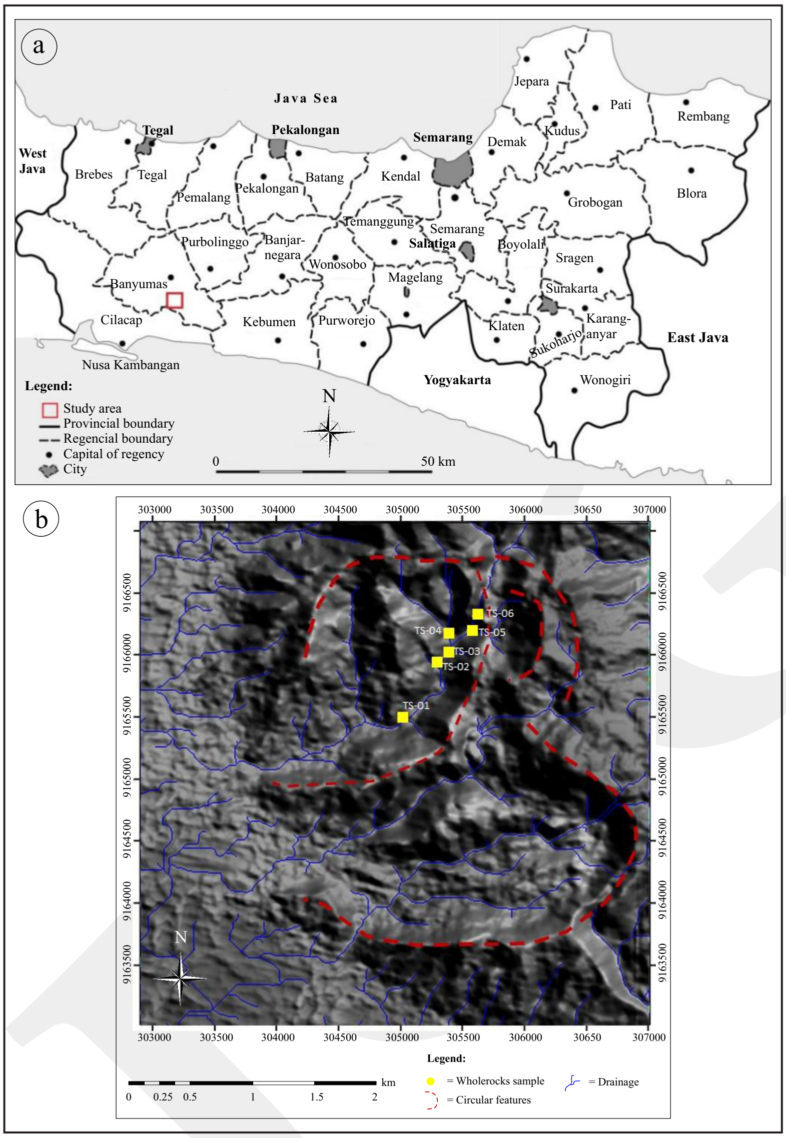

Figure 1. Locality map of: a). The studied area (Kebasen) in 25 km^2, showing b). Morphology of a circular features and a radial drainage pattern.

is the peak of geanticline on Java Island with a trend pattern relatively west-east, covering the area of northern Cilacap, southern Banyumas, southern Banjarnegara, Kebumen, Wonosobo, and Purworejo (Bemmelen, 1949).

According to Asikin *et al*. (1992) in a 1:100.000 scale map, Kebasen is composed of Halang Formation and a member of Halang Breccia. The evidence of volcanic product in Halang Formation is still debatable among Indonesian geoscientists, especially about the genesis of this formation. However, the abundance of volcanic product such as volcanic breccia, tuff, and lava in the studied area is relevant to the results of geophysical study as mentioned by Purwasatriya *et al.* (2017). The result comes to the existence of Mio-Pliocene magmatic arc (volcanic arc) of South Serayu Mountains, especially in Banyumas Basin using the geological subsurface mapping concept with residual gravity data.

Detailed petrogenesis studies of basaltic lava in the Halang Formation, Banyumas Basin, are still very limited. This becomes the reason for further studies. This study aims to understand the genesis of basaltic lava and to determine the geo-tectonic conditions as well as the possibility of sedimentary recycling input and oceanic slab role in tholeiitic magmatism. The results of this study can hopefully be a benefit for mineral, oil, and gas exploration in Banyumas Basin.

Basaltic lava can be produced by almost all tectonic systems, both convergent and divergent, which corresponds to a mid-oceanic ridge or rift in the middle of continental plates with different volcanic characteristics and magma series (Wilson, 1989). A different tectonic system can also produce basaltic lava with different magma affinities, for example: oceanic rifting can produce tholeiitic and alkaline basalts, continental rifting can produce tholeiitic, alkaline, and peralkaline basalts, subduction zones can produce calc-alkali and tholeiitic basalt, and intraplates can produce tholeiitic, alkaline, and peralkaline rocks (Best, 1982).

Based on the ratio between the elements of K_2O, Na_2O, and SiO_2, basaltic lava can be divided into two types, namely alkali basalt and sub-alkali basalt (high alumina/calc-alkali and low-K/tholeiitic basalt) (Middlemost, 1975). Tholeiitic basalt is an extrusive as well as an intrusive products which can be presented in several tectonic systems, such as volcanic-arc basalt (low-K tholeiitic), ocean floor basalt (tholeiitic), ocean island basalt-seamount (tholeiitic), and continental rift basalt-continental flood basalt (tholeiitic) (Wilson, 1989).

Tholeiitic basalt is an extrusive igneous volcanic rock that is low in silica content, dark in colour, low potassic, and comparatively rich in iron and magnesium. In general, it contains mineral such as Ca-plagioclase (labradorite), (Mg, Fe)-pyroxene (ortho-clinopyroxene; poor Ca), and sometimes olivine or quartz. Tholeiitic magma can be generated from the tectonic of oceanic environment {mid-ocean ridge (MOR), island-arc (IA), seamount or ocean island from intra-oceanic}, Active Continental Margin (ACM) or intracontinental-rift (Pearce and Cann, 1973; Wilson, 1989; see in Figure 2).

Based on the geochemistry of major oxides, the tholeiitic magma can be divided into high-Mg primitive tholeiitic (komatiitic), high-Mg primary tholeiitic (primary magma), and high-Fe differentiated tholeiitic (Jensen, 1976). Tholeiitic magma can also be distinguished based on the ratio of La/Yb < 3. Sometimes, the ratio of La/Yb in the range of 3 to 6 can also represent the presence of tholeiitic magma (Barrett and MacLean, 1999).

Geotectonically, it is quite difficult to distinguish the tholeiitic volcanic island-arcs (IAB) from ACM, especially using major oxides with ternary diagram such as in Mullen {1983; (MnOx10)-(P_2O_5x10)-(TiO_2) (wt.%)}; Pearce *et al*. {1975; K_2O-P_2O_5-TiO_2 (wt.%)}; diagram of Pearce *et al*. {1977; MgO-Al_2O_3-FeO(t) (wt.%)}; Irvine and Baragar {1971; (Na_2O+K_2O)-FeO(t)-MgO (wt.%)} or the binary diagram, *e.g*. Miyashiro {1974; FeO(t)/MgO *vs*. SiO_2, (wt.%)}. This is due to the concentration of major oxides of tholeiitic island-arc and tholeiitic ACM that relatively have similar values. The use of isotope ratios of 143Nd/144Nd *vs.* 87Sr/86Sr brings up the difficulties in tholeiitic discrepancies between IA and ACM (Wilson, 1989; Nelson, 2011). Thus, it is difficult to get geochemical data on journals related to a continental-arc tholeiitic. New methodological development with diagram model which involves trace elements, such as HFSE (Zr-Hf, Nb-Ta, Th-U, Ti) and a few elements from REE (such as La, Ce, Sm, Eu, Yb, Y) or total REE (TREY) becomes a better and more precise solution in interpreting the geotectonics.

Continental volcanic-arc (or ACM-arc) is a very complex subduction type, since it involves an oceanic plate (slab) which has a different trace element characteristic with a continental plate.Additionally, there is an implication of sediment melting, subcontinental lithospheric mantle (SCLM), and mantle plume (asthenosphere) which also have different geochemistry characteristics. Some partial melting types were proposed by several authors for the subduction of an oceanic plate towards the continental plate (Table 1). A subduction zone of volcanic arc in Java Island generally involves sediment recycling (Ben Othman *et al.*, 1989; Plank and Langmuir, 1998; Gasparon and Varne, 1998; Turner and Foden, 2001; Gertisser and Keller, 2003; Handley, 2006; Handley *et al*., 2007; Sendjaja *et al*., 2009). However, Krakatau Volcano dan Galunggung

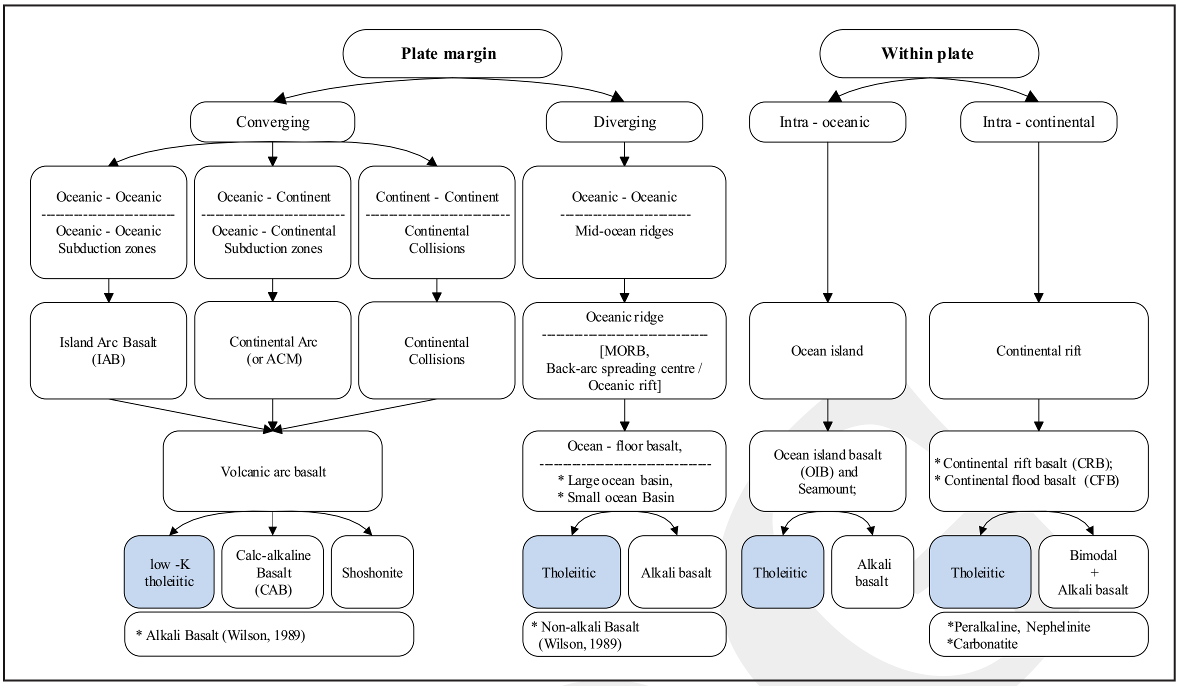

Figure 2. Basalt Tectonic Environment Classification (modified after Pearce and Cann, 1973; Wilson, 1989).

Table 1. Partial Melting from Various Subductions between Oceanic Plate and Continental Plate

No	Subduction Between Oceanic Plate and Continental Plate	Partial Melting Occurs on:	Example
1	As a result of dehydration from the oceanic subduction slab	Lower continental crust	*The lower crust melt (Rudnick and Gao, 2003)
2	As a result of dehydration from the oceanic subduction slab	Lower continental crust (or lower ACM crust) and contaminated with rutile-melt	Sukadana continental flood basalt, Lampung, Sumatra (Zulkarnain, 2011)
3	As a result of dehydration from the oceanic subduction slab	Subcontinent lithoperic mantle (mantle wedge)	The example cases have not yet been compiled.
4	As a result of dehydration from the oceanic subduction slab	Mixing between subcontinental lithospheric mantle (mantle wedge) and ACM crust	High-Mg tholeiitic mantle of Galunggung volcano (Dempsey, 2013)
5	As a result of dehydration from the oceanic subduction slab	Mixing between sediment in the slab (SED) and ACM crust	Merapi Volcano, Yogyakarta (Gertisser and Keller, 2003), Sungai Medanas lava, Karangsambung, Kebumen, Central Java (Ansori, 2007)
6	As a result of dehydration from the oceanic subduction slab	Mixing between SED, ACM crust, and subcontinental lithospheric mantle	The example cases have not yet been compiled.
7	As a result of dehydration from the oceanic subduction slab and continental rifting	Mixing between sediment in the slab (SED), ACM crust, and astenosphere	Ponjen Kalisoka tholeiitic lava, Central Java (Fadlin *et al*., 2018)
8	Oceanic slab melting	Mixing between oceanic crust and continental crust	The example cases have not yet been compiled.
9	Oceanic slab melting	Mixing between oceanic slab, SED, and ACM crust	*This Study
10	Oceanic slab break-off (slab window) or continental rifting	Mixing between continental crust and astenosphere	Krakatau Volcano, West Java (Gardner *et al,* 2013)
11	Oceanic slab break-off (slab window)	Mixing between asthenosphere, subcontinental lithospheric mantle, and continental crust	The example cases have not yet been compiled.

Volcano (West Java) are among few volcanoes which are not contaminated by sedimentary recycling.

Materials and Methods

Six representative samples of pillow lava were taken for laboratory analyses from the Kali Song River. Laboratory analyses of the samples include the petrography and geochemistry analyses. Petrography analysis was done at Petrology-Mineralogy and Environmental Geology Laboratory of Geological Engineering Department of Jenderal Soedirman University by using a polarization microscope. Geochemistry analysis which includes major oxides, trace elements, and rare-earth elements (REE) was done at Intertek Laboratory Jakarta by using the XRF + LOI method and ICP-MS method with a lower detection limit by using four acids which digest in teflon tube. The ICP-MS used the 4A/MS and 4A/OE method for trace elements and ICP-MS 4A/MS11 method for REE elements.

Result of Study

Geological Condition of Studied Area

Morphologically, the studied area shows a slope pattern of the hillside, while the vicinity of the central eruption is steeper than the slopes as it goes away from the centre. It also has a circular feature and drainage pattern that represent a radial pattern (Figures 1, 3). Furthermore, that condition can be interpreted as a characteristic of central

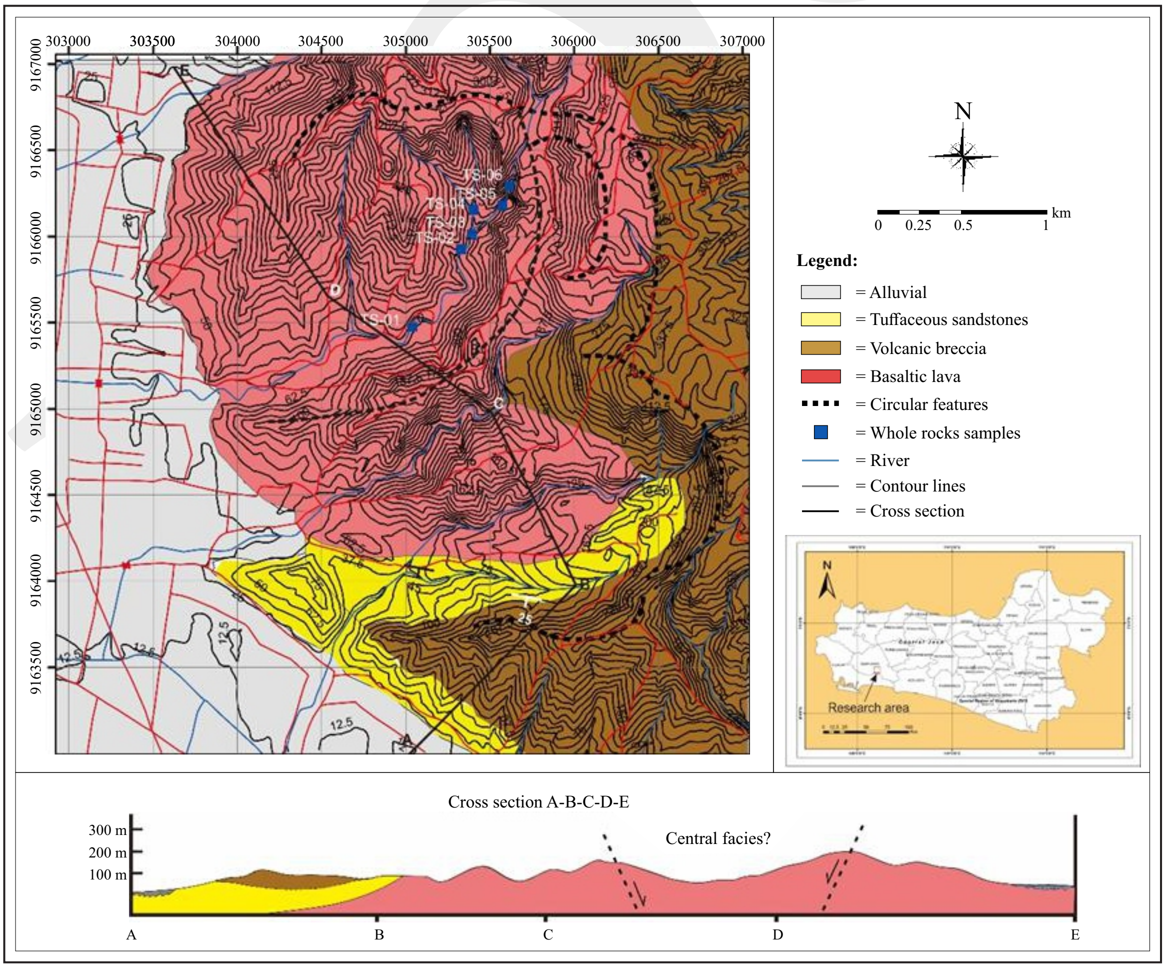

Figure 3. Geological map showing the distribution of lithology units in the studied area which from oldest to youngest: basaltic lava, volcanic breccia, tuffaceous sandstone, and alluvial deposits.

eruption of a Paleo-volcano with a high level of erosion (Bronto, 2006). The stratigraphy of the studied area can be classified into four lithological units, from oldest to youngest: basaltic lava, volcanic breccia, tuffaceous sandstone, and alluvial deposits (Figure 3).

Petrology of Kebasen Pillow Lava

Megascopically, six samples of pillow lava (TS-01; TS-02; TS-03; TS-04; TS-05; and TS-06) are light gray to dark gray colour, aphanitic-porphyroaphanitic texture, showing vesicular texture due to the release of gas during the cooling of magma. Outcrop of the pillow lava shows pillow structure with variegated geometries, which are (a) tabular shape with a multiple rinds, (b) spherical shape alongside with the cross section of the pillow showing the internal radial fracture, (c) irregular shape with the intensity of the colling fracture, (d and e) spherical, oval, and irregular shapes, and (f) megapillow showing the internal radial fractures with the multiple rinds (Figure 4). The multiple rind structure is intensively shown on the outcrops of pillow lavas, indicating that the condition can be controlled by the various factors, such as effusion rate, viscosity, temperature, the total volume of extruded lava, and slope of the underlying surface (Kawachi and Pringle,1988). The appearance of multiple rinds in pillow lava can be assumed that the lava was formed in

Figure 4. Outcrop of Kebasen pillow lava (a=TS-01, b=TS-02, c=TS-03, d=TS-04, e=TS-06, and f=TS-05) showing a pillow structure along the path of Song River with different pillow geometries. (a) Tabular shape with a multiple rinds; (b) Spherical shape with cross section of the pillow showing internal radial fractures; (c) Irregular shape with the intensity of the cooling fracture; (d, e) Spherical, oval, and irregular shapes; (f) Megapillow showing the internal radial fracture with the multiple rinds.

a shallow marine environment (Kawachi and Pringle, 1988).

The observed result using loupe with ten-times of magnification, indicates the samples of basaltic lava which have plagioclase and pyroxene minerals as well as volcanic glass as a rim of the outer part of the pillow structure of the lava body. Based on the results of petrographic analysis of the pillow basaltic lava (TS-01, TS-02, TS-03, TS-04, TS-05, and TS-06), it shows relatively the same characteristics by petrography which is grayish-black in colour, hipocrystalline texture, inequigranular distribution with unique texture porphyritic and intergranular, subhedral-anhedral shapes. All those samples consist of primary mineral such as plagioclase (bytownite-labradorite), pyroxene, hornblende, olivine, and volcanic glass, and also secondary minerals such as opaque, iddingsite, zeolite, carbonate (calcite), and sericite. The occurence of secondary minerals is the evidence that the tholeiitic Kebasen pillow lava exhibits a slightly hydrothermal alteration which is propylitic alteration (Figure 5).

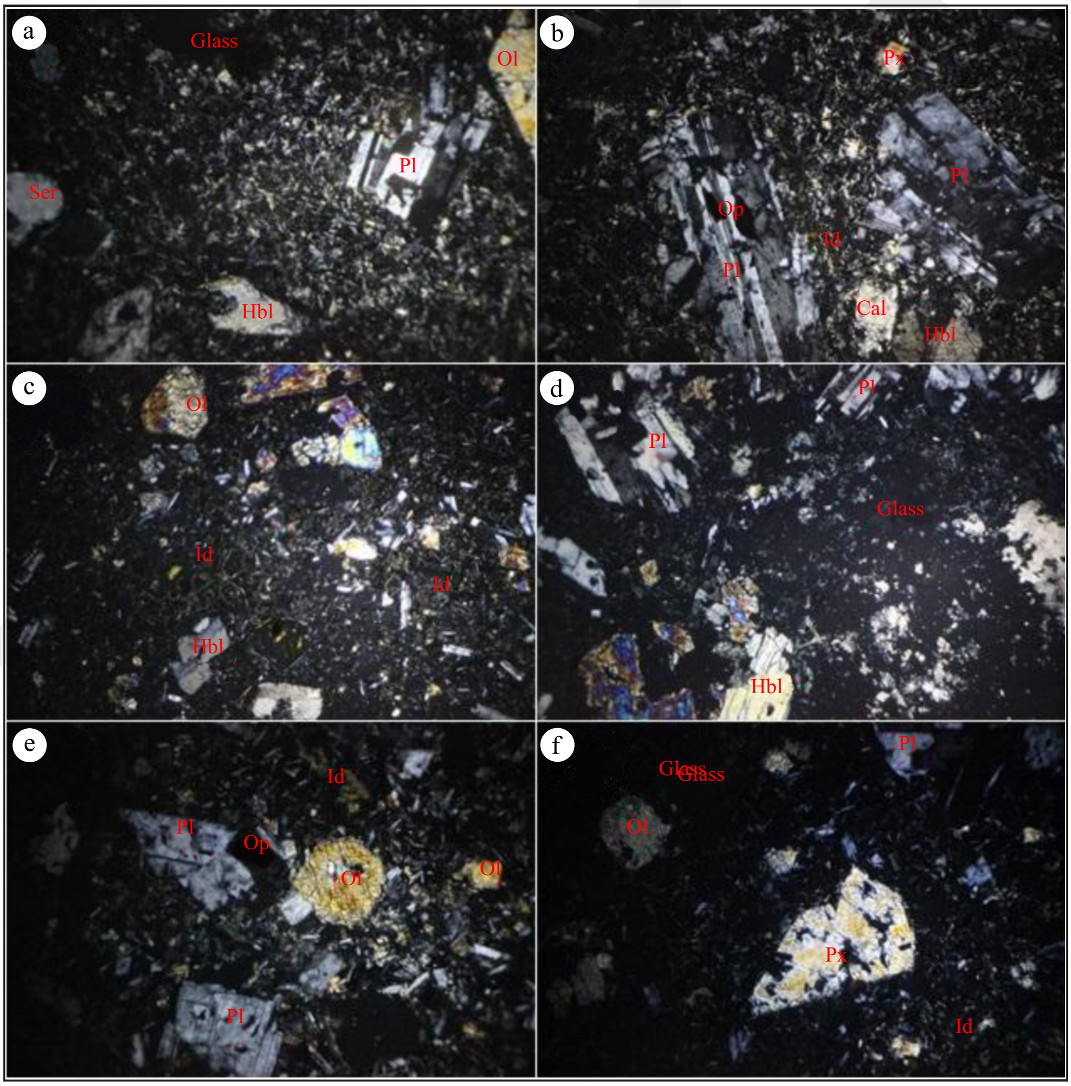

Figure 5. Photomicrographs of Kebasen pillow lava (a=TS-01, b=TS-02, c=TS-03, d=TS-04, e=TS-05 and f=TS-06) consists of primary mineral such as plagioclase (bytownite-labradorite), pyroxene, hornblende, olivine, and volcanic glass, and other secondary minerals {*e.g.* opaque, iddingsite, carbonate (calcite), and sericite}. No free quartz and alkali feldspar mineral found. Mineral abbreviations are adopted from Whitney and Evans (2010) (Pl= Plagioclase, Px= Pyroxene, Hbl= Hornblende, Ol= Olivine and Volcanic Glass, Op= Opaque, Id= Iddingsite, Cal= Calcite, Ser= Sericite).

Geochemical Analysis of Kebasen Pillow Lava

Analysis results of six major oxide geochemical samples presented in Tables 2 show that they relatively have a low LOI value (LOI= 0.43% - 1.46%) except sample TS-04/G (LOI= 3.50%). Major oxide composition ratio based on MIA(o) [{Al_2O_3+Fe_2O_3(t)} *vs*. {(CaO*+Na_2O+K_2O) + MgO}, in molar] in mafic rocks is around MIA(o)= 35.41 - 40.09 far from the 50 boundary which shows that the six samples are fresh rock. MIA (o) is Mafic Index of Alteration (oxidized) referring to the ternary diagram model of Nesbitt and Wilson (1992), modified by Babechuk *et al.*(2014). The Kebasen tholeiitic lava samples are mafic in composition with low SiO_2 contents (48.39-50.66 wt.%), low TiO_2 (0.83 - 0.94 %),

Table 2. Geochemical Analysis Results of Major Oxide Elements of Kebasen Pillow Lavas

Element	Units	Detection limit	TS-01/G	TS-02/G	TS-03/G	TS-04/G	TS-05/G	TS-06/G
Al	PPM	50	87500	86300	86100	88300	85100	91300
Ca	PPM	50	81600	79600	79400	80300	74700	76800
Cr	PPM	5	49	61	103	211	70	46
Cu	PPM	1	148	136	154	136	140	161
Fe	%	0.01	7.17	7.16	6.9	5.5	6.89	7.44
K	PPM	20	4610	3540	3300	8670	3510	4680
Mg	PPM	20	29500	31000	38000	34300	29800	27500
Mn	PPM	1	1550	1220	1660	2520	1110	1150
Na	PPM	20	18600	17100	15400	14000	16600	17400
Ni	PPM	1	37	41	59	83	34	26
P	PPM	50	630	560	540	470	630	670
S	PPM	50	5980	270	420	3160	200	170
Sc	PPM	1	34	33	37	40	32	32
Ti	PPM	5	5330	4860	5040	4870	5200	5540
V	PPM	1	288	285	308	314	298	331
Zn	PPM	1	90	85	86	87	88	93
Ag	PPM	0.1	<0.1	<0.1	<0.1	<0.1	<0.1	<0.1
As	PPM	1	3	2	2	5	2	2
Ba	PPM	1	174	136	174	277	121	142
Be	PPM	0.5	<0.5	<0.5	<0.5	<0.5	<0.5	<0.5
Bi	PPM	0.05	<0.05	<0.05	<0.05	<0.05	<0.05	<0.05
Cd	PPM	0.05	0.08	0.05	0.09	0.1	<0.05	0.08
Co	PPM	1	35	38	38	39	32	30
Cs	PPM	0.1	1.2	0.9	0.3	0.2	0.8	0.9
Ga	PPM	0.1	19.3	19.4	17.5	17.5	18.5	18.8
Ge	PPM	0.1	0.6	0.6	0.7	1.2	1.1	1.1
Hf	PPM	0.1	2	1.9	1.6	1.7	1.7	1.9
In	PPM	0.05	0.05	0.06	0.06	0.05	0.05	0.06
Li	PPM	0.1	4.5	5	7.7	8.5	4.9	6.1
Mo	PPM	0.1	1	0.9	0.5	0.7	0.7	0.7
Nb	PPM	0.1	1.9	1.9	1.4	1.3	1.7	2
Pb	PPM	1	42	13	11	16	9	8
Rb	PPM	0.1	12.2	10	5.4	10.7	6.2	9.4
Re	PPM	0.05	<0.05	<0.05	<0.05	<0.05	<0.05	<0.05
Sb	PPM	0.1	0.2	0.1	0.2	0.2	0.1	0.2
Se	PPM	1	<1	<1	<1	<1	<1	<1
Sn	PPM	0.1	1.1	0.9	0.9	0.9	0.9	1.1
Sr	PPM	0.5	251	248	223	234	233	245
Ta	PPM	0.05	0.2	0.16	0.13	0.12	0.14	0.16
Te	PPM	0.1	<0.1	<0.1	<0.1	<0.1	<0.1	<0.1
Th	PPM	0.05	1.83	1.67	1.4	1.23	1.68	1.88
Tl	PPM	0.02	0.03	0.03	0.05	0.06	0.03	0.04
U	PPM	0.05	0.43	0.39	0.35	1.27	0.34	0.51
W	PPM	0.1	0.3	0.3	0.2	0.5	0.2	0.2

Table 2. continued

Element	Units	Detection limit	TS-01/G	TS-02/G	TS-03/G	TS-04/G	TS-05/G	TS-06/G
Y	PPM	0.1	18.5	19.4	17	18.3	17.7	19.5
Zr	PPM	0.5	59.2	57.9	51.7	50	56.1	60.5
Ce	PPM	0.1	14.3	13.9	11.8	11.7	13.2	15.2
Dy	PPM	0.1	3.2	3.2	2.9	3.2	3	3.5
Er	PPM	0.1	2	2	1.9	2	2	2.2
Eu	PPM	0.1	0.8	0.8	0.7	0.8	0.8	0.8
Gd	PPM	0.1	3.5	3.4	3.2	3.4	3.2	3.6
Ho	PPM	0.1	0.6	0.6	0.6	0.6	0.6	0.7
La	PPM	0.1	6.2	6.1	5.2	5.3	6.1	6.6
Lu	PPM	0.05	0.36	0.34	0.34	0.34	0.3	0.35
Nd	PPM	0.1	8.9	9	8	7.8	8	9.6
Pr	PPM	0.05	1.93	1.84	1.56	1.61	1.79	1.99
Sm	PPM	0.1	2.5	2.5	2.2	2.2	2.2	2.6
Tb	PPM	0.05	0.5	0.5	0.48	0.5	0.52	0.53
Tm	PPM	0.1	0.3	0.3	0.3	0.3	0.3	0.3
Yb	PPM	0.1	1.9	2	1.9	2	2	2.1
Al_2O^3	%	0.01	16.73	16.81	16.34	16.86	16.84	17.37
CaO	%	0.01	11.37	11.44	11.40	11.55	11.14	11.01
Cr_2O_3	%	0.01	0.02	0.03	0.03	0.07	0.02	0.02
Fe_2O_3	%	0.01	10.72	11.01	10.36	8.29	10.86	11.20
K_2O	%	0.01	0.54	0.43	0.39	1.05	0.44	0.56
MgO	%	0.01	5.05	5.52	6.59	5.99	5.39	4.82
MnO	%	0.01	0.23	0.19	0.25	0.37	0.18	0.18
Na_2O	%	0.01	2.44	2.36	2.13	1.90	2.33	2.33
P_2O_5	%	0.002	0.140	0.130	0.122	0.110	0.149	0.153
SiO_2	%	0.01	50.66	50.34	49.69	48.39	50.35	50.35
TiO_2	%	0.01	0.88	0.85	0.87	0.83	0.92	0.94
S	%	0.002	0.589	0.032	0.048	0.329	0.024	0.020
LOI	%	0.01	0.95	0.43	1.46	3.50	0.94	0.95
Total	%	0	100	99.6	99.7	99.2	99.6	99.9

slightly high Al_2O_3 (16.34 - 17.37 %), Fe_2O_3(t) 8.29 - 11.2%, relatively low MgO (4.82 - 6.59 %), relatively high CaO (11.01 - 11.55 %), Na_2O (1.90 - 2.44 %), K_2O (0.39 - 1.05 %), and ratio K_2O/Na_2O (0.18 - 0.55). Moreover, they are low in rubidium (Rb= 5.40 - 12.20 ppm), low niobium (Nb= 1.30 - 2.00 ppm), low tantalum (Ta= 0.12 - 0.20 ppm), relative low zircon (Zr= 50.0 - 60.5 ppm), and low Total REE (TREY= 58.08 - 69.57 ppm). The average percentage of LREE is 50.31% (La--Sm), HREE 49.69% (Eu--Lu+Y), and dEu negative anomaly (dEu= 0.80 - 0.92). The ratio of La/Yb < 3.26, and the ratio of Mg# ranges between 46.0 - 58.9. The definition of slightly high Al_2O_3 and relatively low MgO refers to Kersting and Arculus (1994) for Al_2O_3> 16% are categorized as high-alumina basalt (HAB), and MgO > 7% is high-magnesian basalt (HMB).

The plot results in TAS diagram (after Le Bas *et al.*, 1986) show the six samples of Kebasen pillow lava which have a low total alkali content (Na_2O+K_2O= 2.52 - 2.98%) falling in sub-alkaline field (Figure 7). The sub-alkaline field in this TAS diagram can be indicated in the form of tholeiitic series or calc-alkaline series. In order to ensure which type of series is more appropriate, plotting was carried out by involving the multicationic diagram of De la Roche *et al.* (1980). The plotting result shows the six samples of Kebasen lava is confirmed as a tholeiitic rock (Figure 8). This interpretation is supported by using diagram model from Miyashiro (1974) (subdiscrimination in Figure 9). Plotting result of Kebasen tholeiite which has SiO_2 with the range of 48.39 - 50.66 wt.%, relatively low Mg# (46.02 - 58.87), and it has a negative dEu anomaly attribute (dEu= 0.80 - 0.92). It indicates that

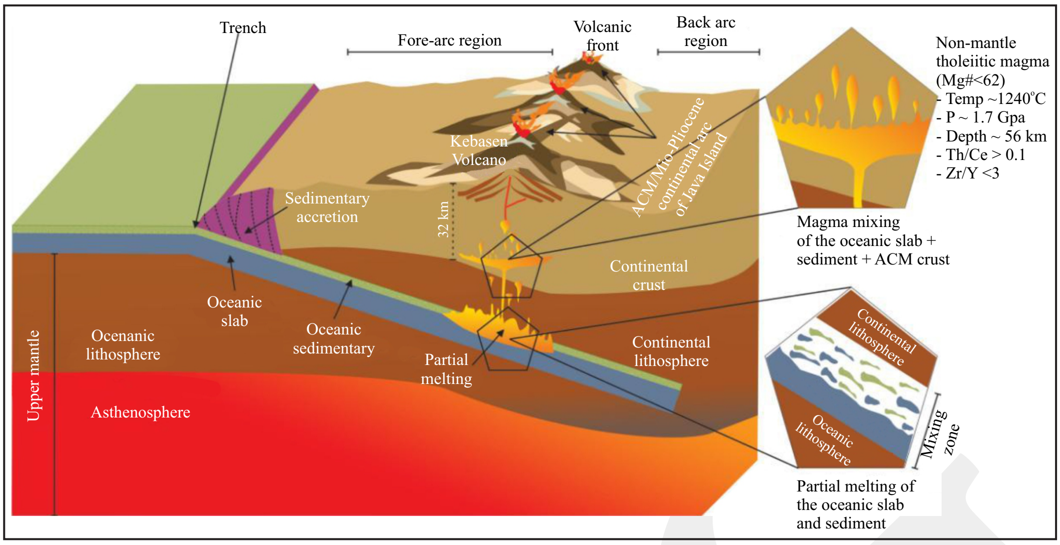

Figure 6. Cartoon illustrating the geotectonic setting of tholeiitic ACM on Kebasen area (Central Jawa). Th/Ce > 0.1 is the signature of oceanic sediment recycling input (after Hawkesworth *et al*., 1997 and after He *et al*., 2008). Zr/Y < 3 is the representative of constituent of oceanic crust (Pearce, 1983 in Figure 9; see also Figure 8).

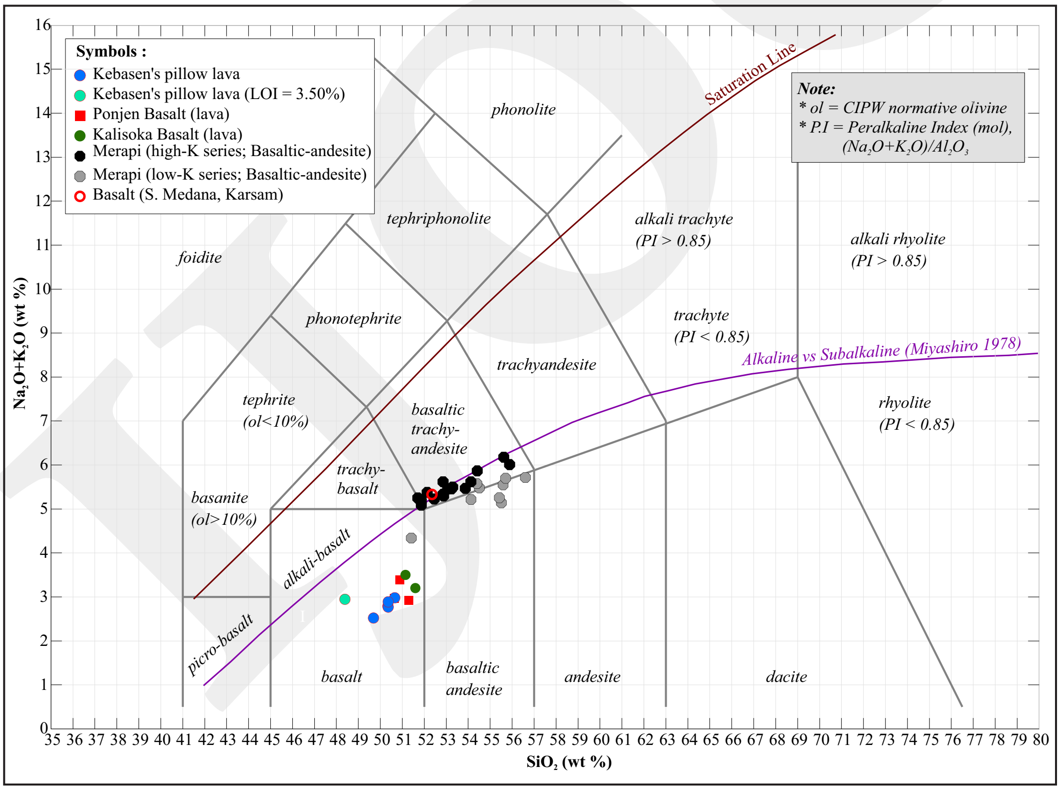

Figure 7. TAS Diagram (after Le Bas *et al*., 1986). Plotting without normalized LOI.

the six Kebasen lava samples are differentiated tholeiitic rock (nonmantle tholeiitic; see in Figure 9). Furthermore, it can be interpreted the magmatism of Kebasen tholeiite has limited involvement of mantle wedge (subcontinental lithospheric mantle; SCLM). As a comparison is the Galunggung high-Mg tholeiitic (West Jawa; Dempsey, 2013; data on page 240) where it has a high concentration of MgO (10.11 - 10.33%) and high value Mg# ~66.4 (Figure 11) with mantle

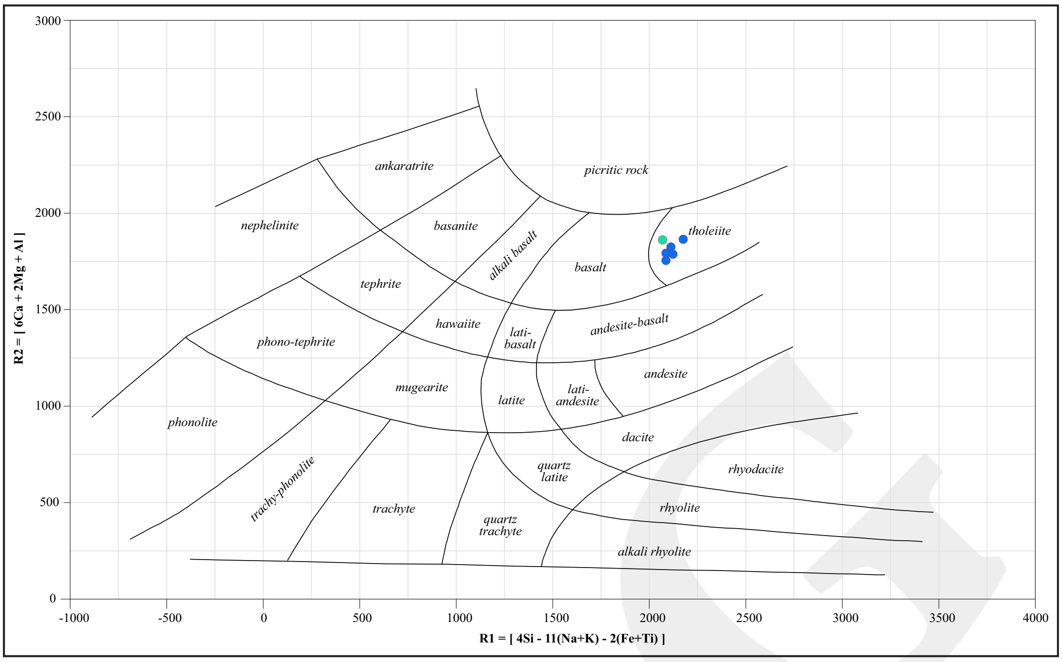

Figure 8. Igneous Rocks classification diagram, R1-R2 multicationic (after De la Roche, 1980).

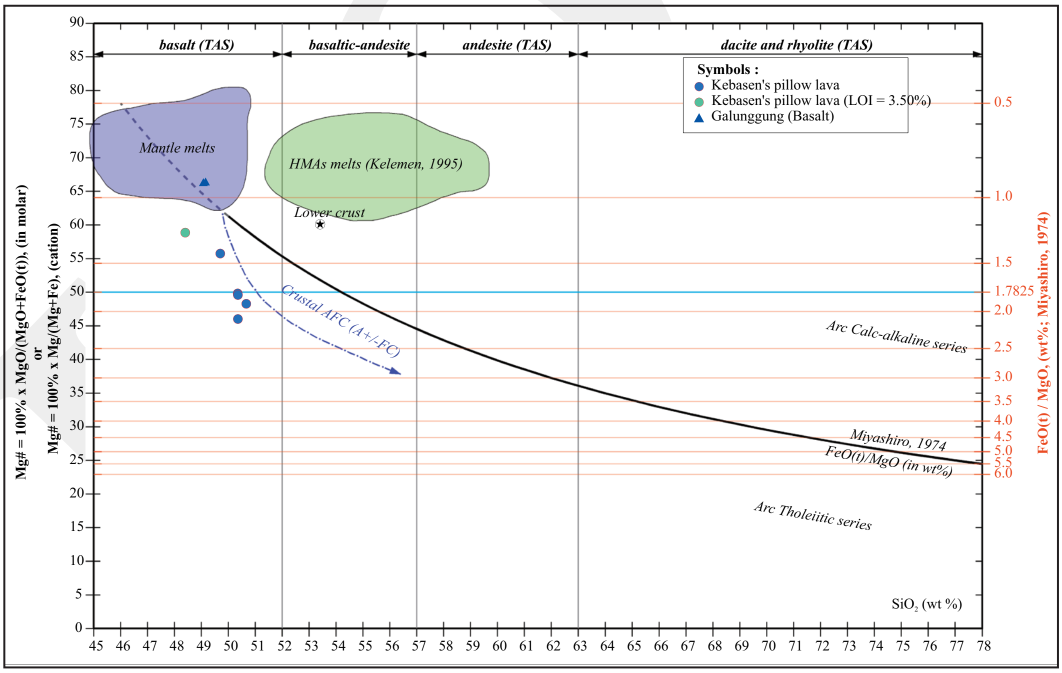

Figure 9. Index of differentiation diagram (Mg#; after Schilling *et al*., 1983). mantle-melts is taken from Kinzler (1997), crust-melts (Dokuz, 2011), high-Mg andesites melts (HMAs; Kelemen, 1995). The discrimination of magnesian series *vs*. ferroan series (Frost and Frost, 2008). The black solid line is mathematically converted from Miyashiro (1974) for discriminating Arc Calc-alkaline *vs*. Arc Tholeiitic series.

wedge partial melting as well as dEu with positive anomaly attribute (dEu= 1.01 - 1.03).

The trace element plotting by using the diagram from Hollocher *et al*. (2012) (Figure 10) and Pearce and Norry (1979), Pearce (1983) (Figure11) shows a transition from oceanic arc towards ACM arc. The results of the plot on this diagram reveal the typical subduction

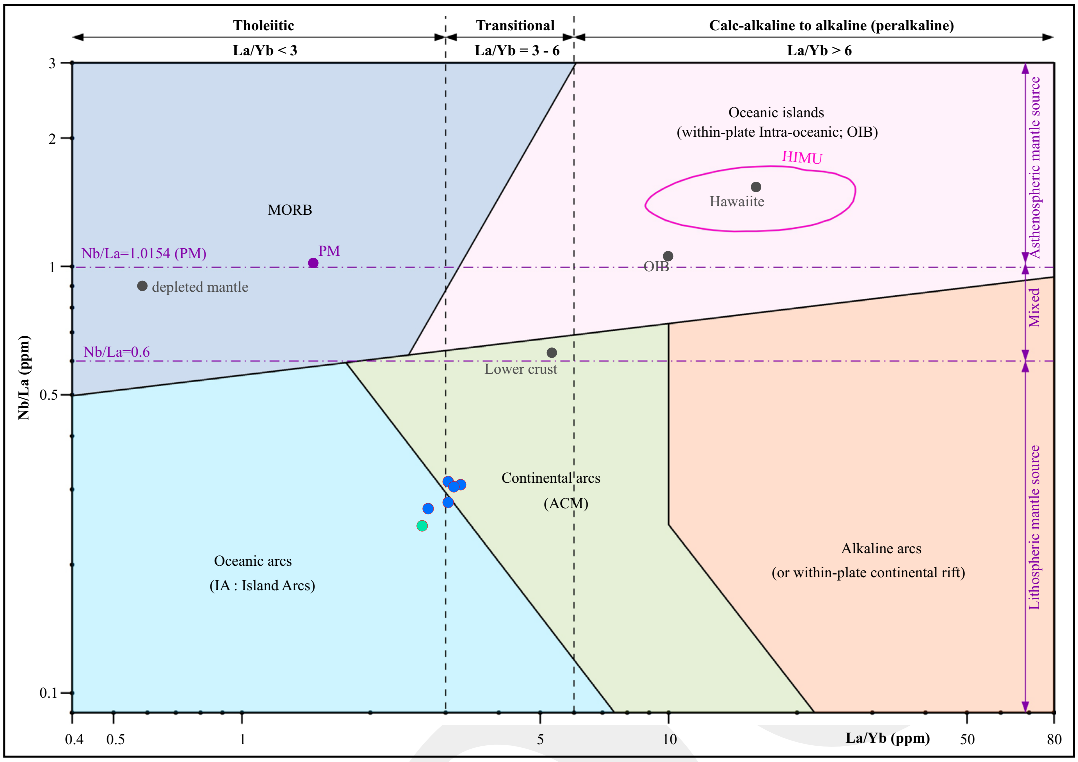

Figure 10. Tectonic discrimination diagram for Basalts (after Hollocher *et al*., 2012a). Magmatic Affinity: ratio La/Yb for Tholeiitic--Transitional--Calc-alkaline to Alkaline (MacLean and Barrett, 1999); the ratio Nb/La for Lithospheric and Asthenospheric mantle is adopted from after Abdel-Rahman (2002). The plot shows Kebasen tholeiitic is formed from the melting of the oceanic slab to continental plate, which is represented by the contribution of trace elements from oceanic crust to continental (ACM).

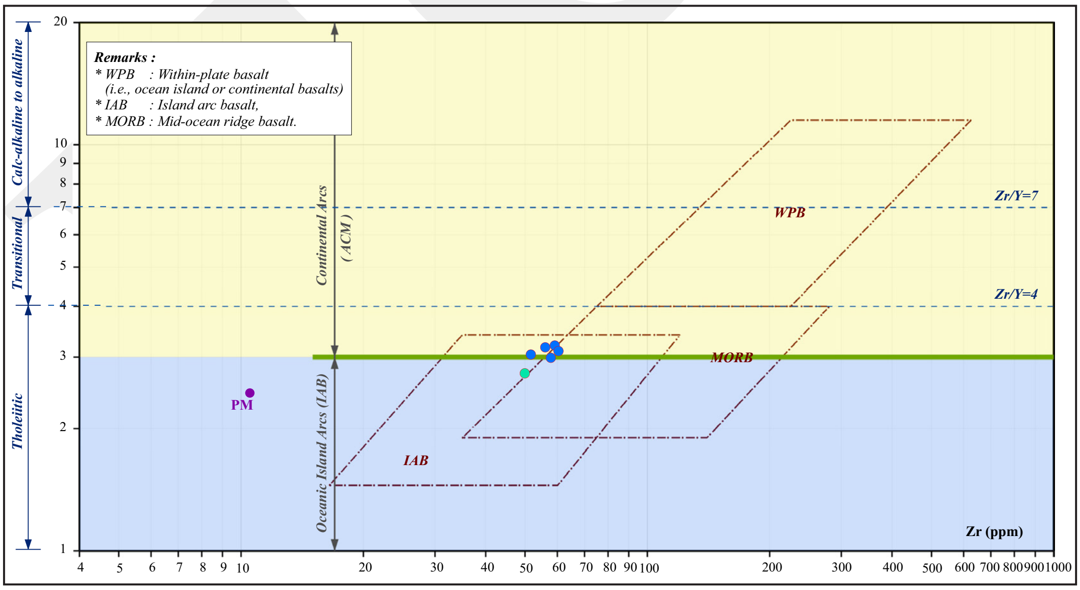

Figure 11. Basalts discrimination diagram of IAB–MORB–WPB (Pearce and Norry, 1979), and the discrimination diagram for Continental Arcs (ACM) *vs*. Oceanic Island Arcs (IAB) (Pearce, 1983b). Determination of Magmatic Affinity: the ratio of Zr/Y for Tholeiitic--Transitional--Calc-alkaline to Alkaline (MacLean and Barrett, 1999).

between the oceanic plate and a continental plate, in which there is a melting on the oceanic slab. Furthermore, it could be interpreted that there are contributions of trace elements from oceanic slab in ACM Kebasen tholeiitic magmatism.

The diagram modeling for element transfer from subducted crust (slab) was developed by Hawkesworth *et al.* (1997) and He *et al.* (2008) with the ratio of Th/Ce= 0.1 as minimum cut off for sediment melting of modern arcs. In this study, the development ratio of Th/Ce during magmatic differentiation was considered. Therefore, the contamination of sedimentary recycling is limited only to SiO_2 < 57% (max basaltic-andesite) condition. As an illustration, plotting to the lower, middle, and upper crust (data from Rudnick and Gao, 2003) was done and could be clearly seen that the ratio Th/Ce for middle crust (Th/Ce= 0.1226) and upper crust (Th/Ce = 0.1667) had exceeded the cut off limit 0.10. In this case, the increase of Th/Ce ratio at middle and upper crust is not related to the enrichment element from the sedimentary recycling input, but it comes from the compositional trend. Plotting result on diagram Th/Ce (in ppm) *vs.* SiO_2 (wt.%) (Figure 12) for Kebasen tholeiite with a range of Th/Ce 0.1051 - 0.1280 shows that there is contamination from oceanic sediment recycling input. As a comparison, there are data from the MORB Bompoka Island (Andaman Sea, India Ocean; Jafri and Sheikh, 2013), where the ratio Th/Ce is far away from the 0.1 boundary. Likewise IAB from Barren Island (Andaman Sea; Chandrasekharam *et al.*, 2009), Galunggung ACM tholeiite (West Jawa; Dempsey, 2013), Anak Krakatau Volcano (ACM; Gardner *et al.*, 2013) including the magmatism do not involve the sediment recycling (see in Figure 13).

The plotting of sample that represents magma (TS-03/G) with the least magmatic evolution has a relatively high magnesium concentration (MgO: 6.59%). The plot of T(°C) *vs.* MgO (wt.%) diagram shows the melting temperature occured at 1243 °C (Ghiorso and Sack, 1995; Asimow *et al.*, 2001) on subdiscrimination (Figure 14). The

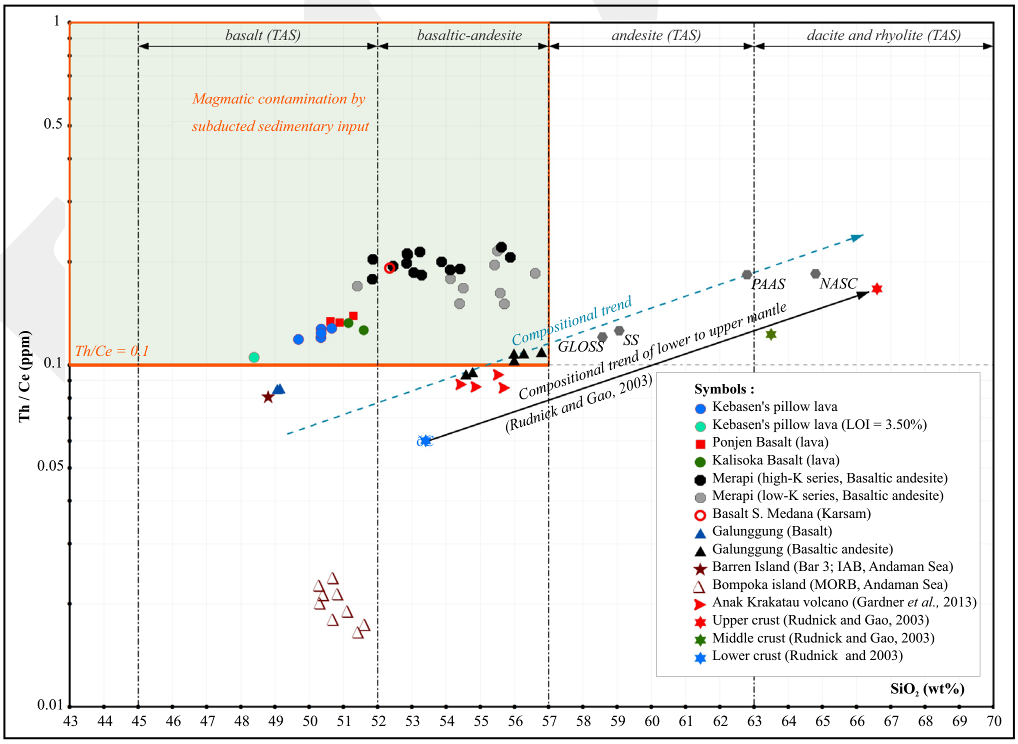

Figure 12. Magmatic contamination by Subducted Sedimentary Input Diagram (after Hawkesworth *et al.*, 1997; after He *et al.*, 2008). The cutoff at Th/Ce=0.1 is the lower limit for modern arcs with an input from sediment melting. The magma of Galunggung volcanics is interpreted without involving the sedimentary recycling, because the Galunggung basalt has a ratio of Th/Ce ~ 0.085 below 0.1; whereas Kebasen tholeiitic involves the sediment recycling. GLOSS (Global Subducting Sediment; Plank and Langmuir, 1998), SS (Silicic sediments; Gasparon and Varne, 1998), PAAS (Post-Archean Australian Shale; Taylor and McLennan, 1985), NASC (North American Shale Composite; Gromet *et al.*, 1984).

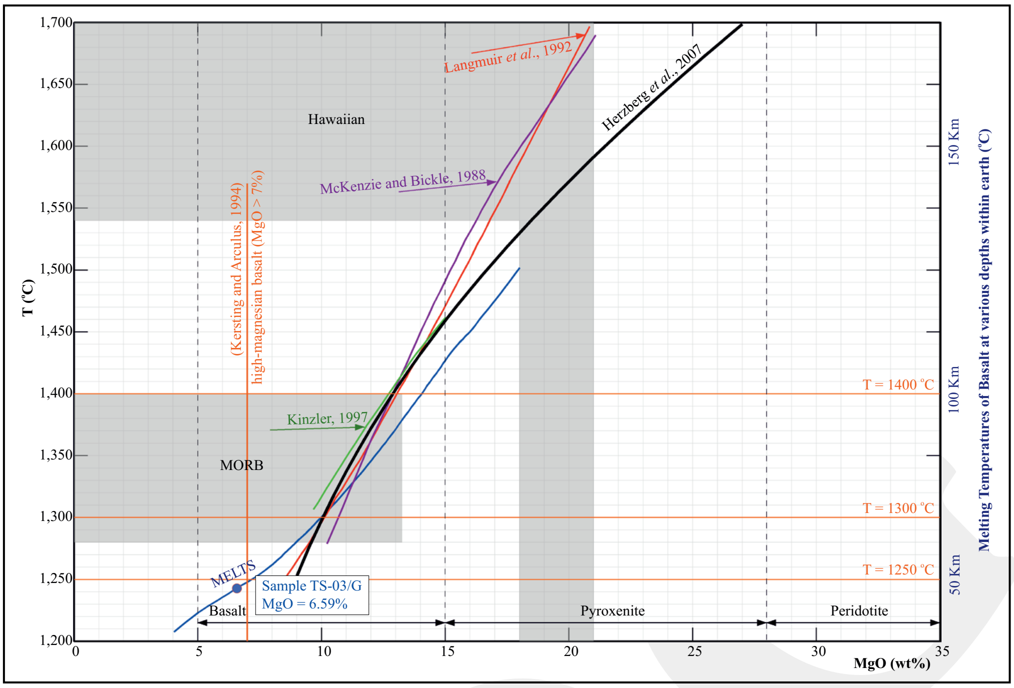

Figure 13. Mantle potential temperatures (Tp, °C) as a function of the MgO concentrations of primary magmas (after Herzberg *et al.,* 2007). MELTS blue solid line (Asimow *et al*., 2001). The plot shows the melting temperature of Kebasen tholeiitic rock (sample TS-03/G) occur at 1243°C.

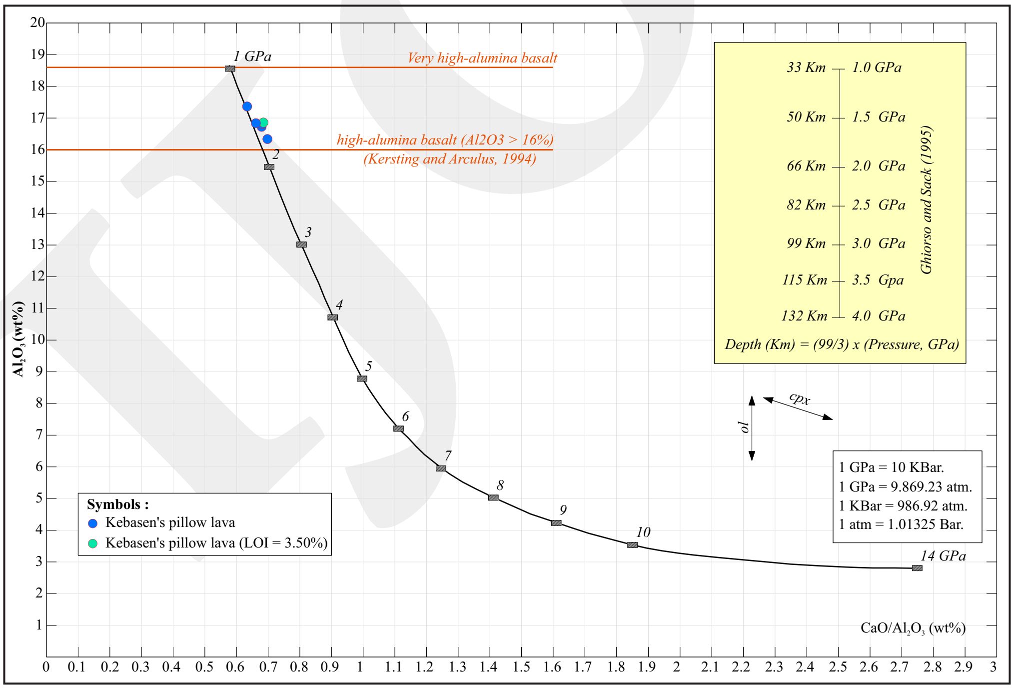

Figure 14. Pressure of Magmatic Segregation Diagram (Herzberg, 1995). Al_2O_3 *vs*. CaO/Al_2O_3 in wt.%. The plots show the melting pressure of Kebasen tholeiitic rock at around 1.7 GPa (17 KBar) with a depth of ~ 56 km.

plot result for the pressure of magmatic segregation on a diagram of Herzberg (1995) shows the melting of magma occured at the pressure of around 1.7 GPa (17 KBar), and correlation between pressure and depth of ~56 Km (Ghiorso and Sack, 1995)on subdiscrimination (Figure 15).

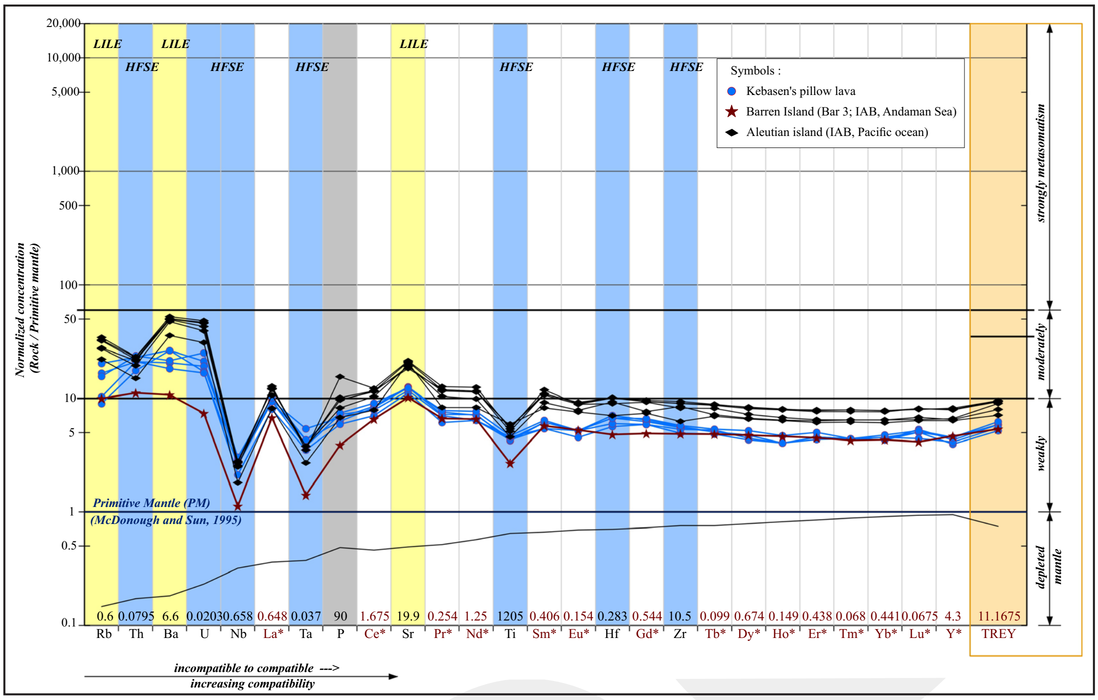

Figure 15. Incompatible to compatible multi-trace elements diagram Normalized to Primitive Mantle (the incompatibility sequence: after Zhang, 2014). The description of weakly-moderately-strongly mantle metasomatism is only used for the determination of metasomatism level of mafic rocks (modified from Godang *et al.,* 2016). Primitive Mantle (PM) values are taken from McDonough and Sun, 1995 and Depleted Mantle (DM) from Salters and Stracke, 2004. The spidergram of Kebasen ACM tholeiite (this study), Tholeiitic-IAB of Barren Island (Chandrasekharam *et al*., 2009), and Tholeiitic-IAB Aleutian Island (northern Pacific Ocean) have a relatively same pattern.

Discussions

The significant presence of various geometries of pillow lavas is influenced by the volume of extruded lava, and the slope of the underlying surface. The accumulation of lava flows with different extrusive volumes and surface slopes will produce dissimilar geometric models of pillow lavas (Schnur, 2007). The existence of the dominant vesicles with a variety of sizes in pillow lava samples mostly filled by zeolites, carbonate minerals, and maximally dissolved of gases by relatively small of hydrostatic pressure is the evidence that basaltic lava was formed in a shallow marine.

The classification of the extrusive igneous rocks refers to the composition of the rock-forming minerals QAP (Quartz-Alkali Feldspar-Plagioclase; Streckeisen, 1978). The six samples of pillow lava are identified as basalt which no free quartz and alkali-feldspar. It can be assumed that the ratio of 'free quartz and alkali feldspar' against plagioclase (QA:P) is 0:100 (see Figure 5). The evolution of plagioclase in Kebasen magmatism is not really significant. It is only in the form of decreasing of calcic- concentration in the plagioclase system (bytownite evolves into labradorite) which is controlled by normal differentiation of the magma (crystal fractionation). The existence of the secondary minerals such as iddingsite, zeolite, calcite, and sericite in those pillow lavas can be interpreted as a product that occurs because of the low-temperature hydrothermal process (Talbi dan Honnorez, 2003). The sample of TS-04/G (LOI= 3.50%) is an exact indication that they are subjected to slightly hydrothermal alteration, where the olivine is the mineral which most easily altered in pillow lava into iddingsite mineral (Talbi dan Honnorez, 2003). The other secondary minerals like zeolite is a change from volcanic glass, whereas sericite and calcite minerals are from Ca-plagioclase (*e.g*. bytownite, labradorite) (Gifkins *et al*., 2005). In this case, the conditions of the hydrothermal system that controls the formation activity and the depth of the environment for the formation of the pillow lava in the studied area cannot be explained in detail due to data limitations. However, based on the texture of the pillow lava, which is dominantly small size in diameter, the formation of basaltic pillow lava may occur at a shallow marine (submarine volcano) with a low pressure control. The use of igneous rock geochemistry diagram such as Pearce and Norry (1979) and Pearce (1983) (Zr/Y *vs*. Zr) is quite difficult to discriminate the tholeiitic volcanic arc which is formed from ACM or island arc (IA), because it points to the same shadowing. Furthermore, the spider diagram also shows a relatively same pattern. This is probably due to the tholeiitic arc with low concentration of the trace elements and REE {TREY < 10x PM (Primitive Mantle); Godang *et al*., 2016}. For example, plotting a comparison of spider digram between Kebasen tholeiitic-ACM (this study), tholeiitic-IAB Barren Island (Chandrasekharam *et al.,* 2009), and tholeiitic-IAB Aleutian Island (northern Pacific Ocean; http://georoc.mpch-mainz.gwdg.de), where those three shows a relatively same pattern (Figure 15).

In this study, the Ponjen-Kalisoka tholeiitic *vs*. Kebasen tholeiitic was compared, where both are formed by the geotectonic setting of ACM. In spider diagram (Figure 16), it is clearly shown that both have the same pattern except the value of Ta (tantalum), which is relatively high in Ponjen-Kalisoka indicating to be contaminated with other magma originating from continental rifting (Fadlin *et al*., 2018).This is the difference between Ponjen-Kalisoka tholeiitic and Kebasen tholeiitic basalts.

Kebasen tholeiitic rocks (basalt lava) have a spidergram pattern of trace elements which is characterized by distinctly negative spikes in Nb-Ta (Figure 17), whereas the spidergram pattern of REE is slightly enriched in LREE (Figure 18).

The considering location of the existence of Kebasen tholeiitic lava is located on the southern end of the Central Java region and

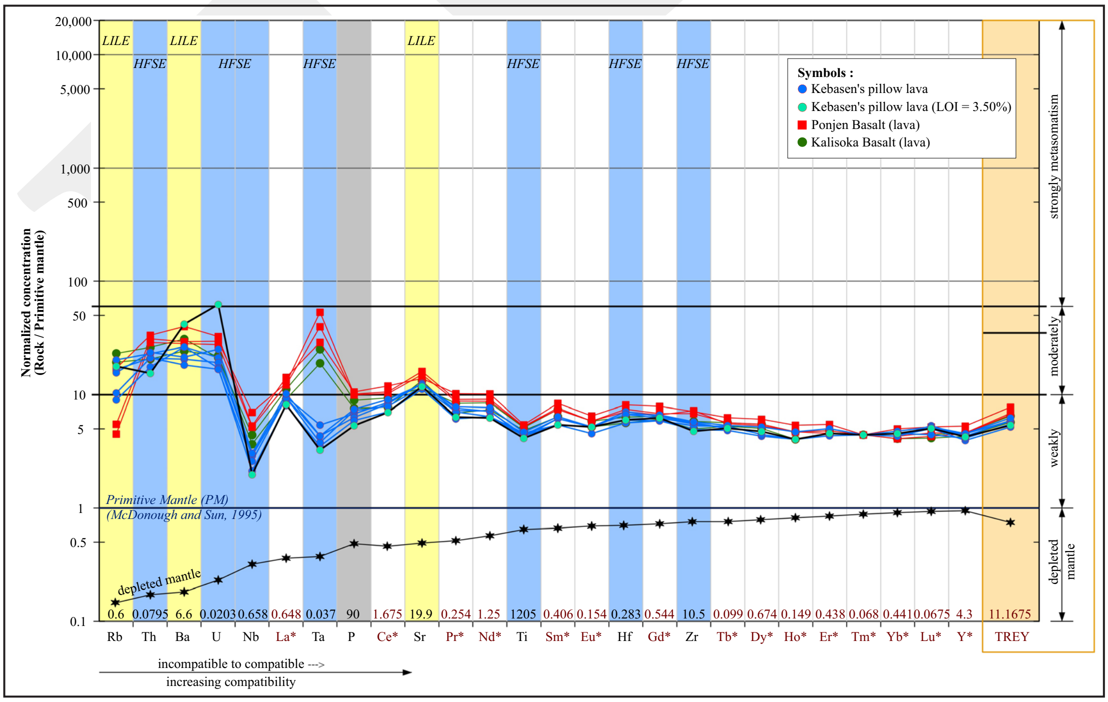

Figure 16. Spidergram of Kebasen ACM tholeiitic (this study) has the same pattern as Ponjen-Kalisoka basalt, except the trend for Tantalum (Ta). The relatively high Tantalum value of Ponjen-Kalisoka (Ta = 0.70 - 1.98 ppm; Fadlin *et al.* (2018), p.22 and p.27) is interpreted to be contaminated with the magma originating the continental-rift.

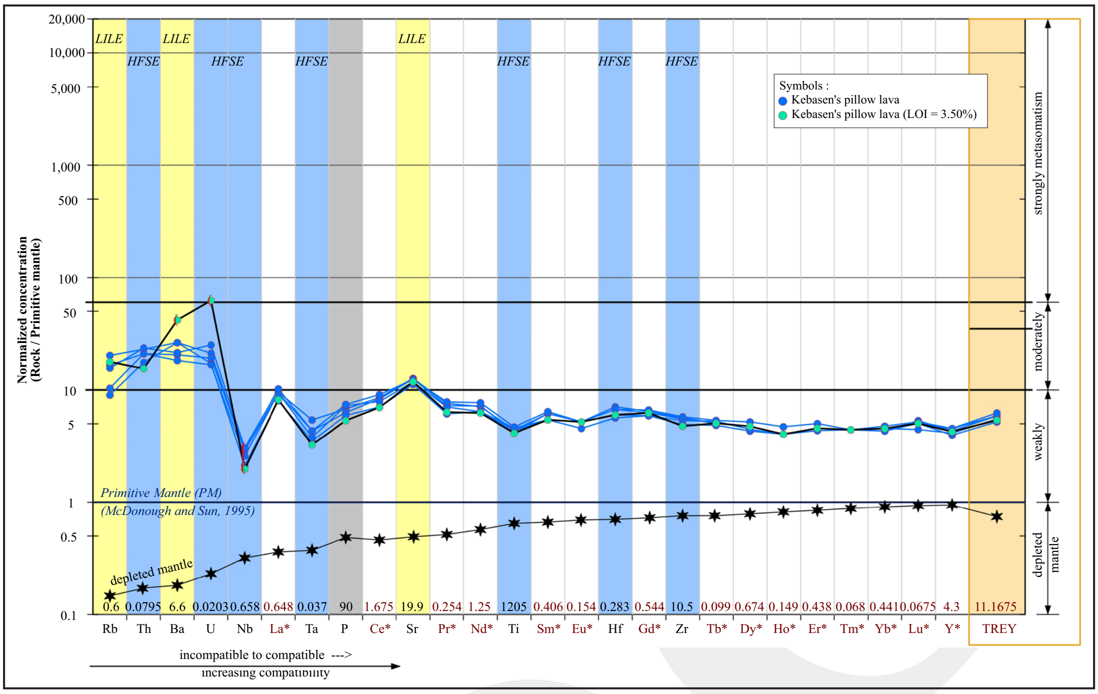

Figure 17. Spidergram of Kebasen ACM tholeiitic (this study) is characterized by distinctly negative spikes in Nb-Ta.

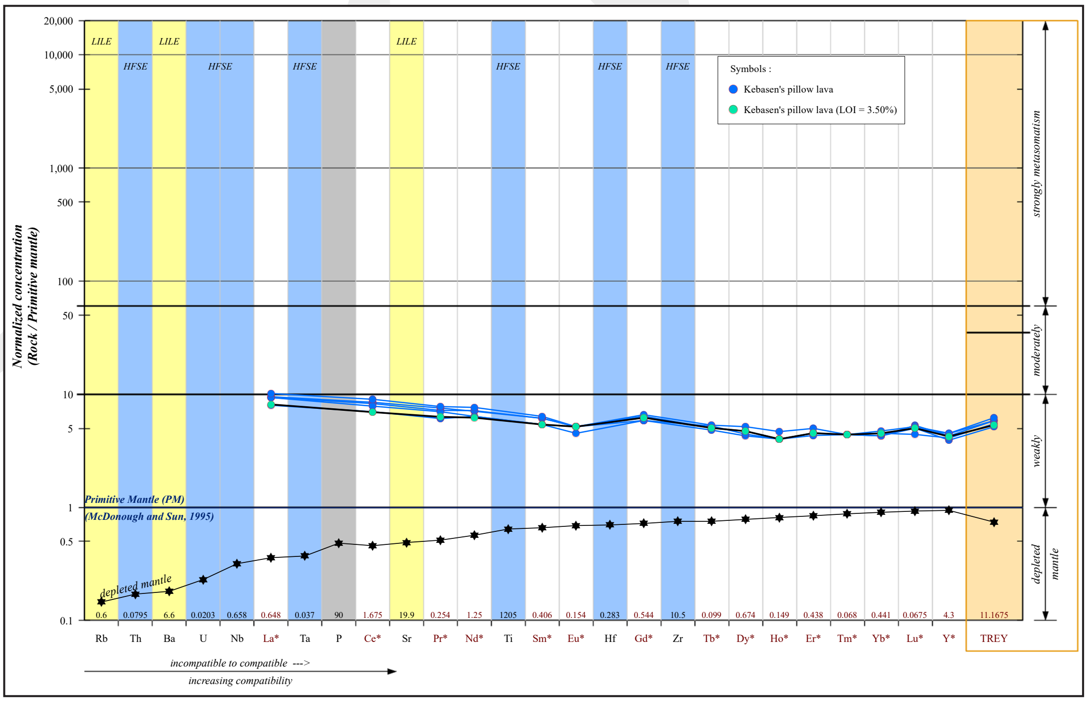

Figure 18. Spidergram REE pattern of Kebasen ACM tholeiitic (this study) has slightly enriched in LREE.

directly facing the trough position of the Indian Ocean. In addition, it also compares the La/Yb ratio value of Kebasen tholeiitic lava (La/Yb < 3.26) which is lower than Ponjen tholeiitic one (northern Serayu; La/Yb ~4.30) (Fadlin *et al*., 2018). Therefore, the Kebasen tholeiitic lava is interpreted as fore-arc ACM-tholeiitic magmatism.

Conclusions

From an integrated study, including petrography, mineralogy, and geochemistry multidiagram plotting (including major oxides, trace elements, and REE of six Kebasen lava samples), it can be concluded as follows:

1. Kebasen pillow lava is identified as basalt with various geometries of pillow structures such as spherical, tabular, oval, and irregular shapes.
2. Kebasen pillow lava is a tholeiitic rock formed by Active Continental Margin (ACM) geotectonic order, involving *sedimentary recycling* as well as the occurrence of trace element input from oceanic-slab melting.
3. Kebasen tholeiitic pillow basaltic lava was due to a fore-arc ACM magmatism.
4. The partial melting conditions are suggested to occur at the temperature of ~1240 ^{o}C and pressure of around 17 KBar at ~56 km depth.

Acknowledgements

The authors express their gratitude to Dr. Arifudin Idrus (Gadjah Mada University) and Eko Bayu Purwasatrya, S.T., M.Si. (Jenderal Soedirman University) for their help, support, and discussion for this manuscript.

References

Abdel-Rahman, A.M., 2002. Mesozoic volcanism in the Middle East: geochemical, isotopic and petrogenic evolution of extension related alkali basalts from central Lebanon. *Geological Magazine,* 139 (6), p.621-640. DOI: 10.1017/S0016756802006829

Ansori, Chusni, 2007. Petrogenesa Basalt Sungai Medana Karangsambung, Berdasarkan Analisis Geokimia. *Jurnal Riset Geologi & Pertambangan,* 17 (1), p.37-50. DOI: 10.14203/risetgeotam2007.v17.143

Asimow, P.D., Hirschmann, M.M., and Stolper, E.M., 2001. Calculation of peridotite partial melting from thermodynamic models of minerals and melts, IV. Adiabatic decompression and the composition and mean properties of mid-ocean ridge basalts, *Journal of Petrology,* 2 (5), p.963-998. DOI: 10.1093/petrology/42.5.963

Asikin, S., Handoyo, A., Prastistho, B., and Gafoer, S., 1992. *Peta Geologi Lembar Banyumas, Jawa Tengah*, *skala 1:100.000*. Pusat Penelitian dan Pengembangan Geologi, Bandung.

Babechuk, M.G., Widdowsonc, M., and Kamber, B.S., 2014. Quantifying chemical weathering intensity and trace element release from two contrasting basalt profiles, Deccan Traps, India.Elsevier, *Chemical Geology,* 363, p.56-75. DO: 10.1016/j.chemgeo.2013.10.027

Barrett, T.J. and MacLean, W.H., 1999. Volcanic Sequences, Lithogeochemistry, and Hydrothermal Alteration in Some Bimodal Volcanic-Associated Massive Sulfide Systems. *Reviews in Economic Geology,* 8, p.101-132. DOI: 10.5382/Rev.08

Bemmelen, R.W.Van., 1949. *The Geology of Indonesia, Vol. 1 A*, Government Printing Office, The Hague, 732pp.

Ben Othman, D., White, W.M., and Patchett, J., 1989. The geochemistry of marine sediments, island-arc magma genesis and crust-mantle recycling. *Earth and Planetary Science Letters,* 94, p.1-21. DOI: 10.1016/0012-821X(89)90079-4

Best, G., 1982. *Igneous and metamorphic petrology*. San Fransisco, Freeman and Company. 758pp.

Bronto, S., 2006. Fasies Gunungapi dan Aplikasinya. *Jurnal Geologi Indonesia,* 1, p.59-71.

Chandrasekharam, D., Santo, A.P., Capaccioni, B., Vaselli, O., Alam, M.A., Manetti, P., and Tassi, F., 2009. Volcanological and petrological evolution of Barren Island. *Journal of Asian Earth Sciences,* 35, p.469-487. DOI: 10.1016/j.jseaes.2009.02.010

De la Roche, H., Leterrier, J., Grandclaude, P., and Marchal, M., 1980. A classification of volcanic and plutonic rocks using R1-R2-diagrams and major element analysis, its relationships with current nomenclature. *Chemical Geology,* 29, p.183-210. DOI: 10.1016/0009-2541(80)90020-0

Dempsey, S.R., 2013. *Geochemistry of volcanic rocks from the Sunda Arc (Durham E-Theses*: Thesis for the degree of Doctor of Philosophy), Data for Galunggung Volcanic, 240pp.

Fadlin, Godang, S., and Hamzah, W.D., 2018. Active Continental Margin (ACM) Origin of Tholeiitic Magmatism in Northern and Southern Serayu-Banyumas, Central Java. *Journal of Geology and Mineral Resources,* 19 (1), p.15-30.

Gardner, M.F., Troll, V.R., Gamble, J.A., Gertisser, R., Hart, G.L., Ellam, R.M., Harris, C., and Wolff, J.A., 2013. Crustal differentiation processes at Krakatau Volcano, Indonesia. *Journal of Petrology*, 54 (1), p.149-182. DOI: 10.1093/petrology/egs066

Gasparon, M. and Varne, R., 1998. Crustal assimilation versus subducted sediment input in west Sunda arc volcanics: an evaluation. *Mineralogy and Petrology,* 64, p.89-117. DOI: 10.1007/BF01226565

Gertisser, R. and Keller, J., 2003. Trace Element and Sr, Nd, Pb, and O Isotope Variations in Medium-K and High-K Volcanic Rocks from Merapi Volcano, Central Java, Indonesia: Evidence for the Involvement of Subducted Sediments in Sunda Arc Magma Genesis. *Journal of Petrology,* 4, (3), p.457-489.

Gifkins, C., Herrmann, W., and Large, R., 2005. *Altered Volcanic Rocks. A guide to description and interpretation*. Published by the Centre for Ore Deposit Research. University of Tasmania, Australia. 275pp.

Ghiorso, M.S. and Sack, R.O., 1995. Chemical Mass Transfer in Magmatic Processes. IV. A Revised and Internally Consistent Thermodynamic Model for the Interpolation and Extrapolation of Liquid-Solid Equilibria in Magmatic Systems at Elevated Temperatures and Pressures. *Contributions to Mineralogy and Petrology,* 119, p.197-212. DOI: 10.1007/BF00307281

Godang, S., Fadlin, and Priadi, B., 2016. Geochemical Signatures of Potassic to Sodic Adang Volcanics, Western Sulawesi: Implications for Their Tectonic Setting and Origin. *Indonesian Journal on Geoscience,* 3 (3), p.195-214. DOI: 10.17014/ijog.3.3.195-214

Gromet, L.P., Dymek, R.F., Haskin, L.A., and Korotev, R.L., 1984. The 'North American Shale Composite': its compilation, major and trace element characteristics. *Geochimica et Cosmochimica Acta,* 48 (12), p.2469-2482. DOI: 10.1016/0016-7037(84)90298-9

Handley, H.K., 2006. *Geochemical and Sr-Nd-Hf-O isotopic constraints on volcanic petrogenesis at the Sunda arc, Indonesia.* Disertation from Durham University.

Handley, H.K., Macpherson, C.G., Davidson, J.P., Berlo, K., and Lowry, D., 2007. Constraining fluid and sediment contributions to subduction-related magmatism in Indonesia: Ijen Volcanic Complex. *Journal of Petrology,* 48 (6), p.1155-1183. DOI: 10.1093/petrology/egm013

Hawkesworth, C.J., Turner, S.P., McDermott, F., Peate, D.W., and Calsteren, P.van, 1997. U-Th Isotopes in Arc Magmas: Implications for Element Transfer from the Subducted Crust. *Science,* 276 (5312), p.551-555. DOI: 10.1126/science.276.5312.551

He, Y., Zhao, G., Sun, M., Wilde, and Wilde, S.A., 2008. Geochemistry, isotope systematics and petrogenesis of the volcanic rocks in the Zhongtiao Mountain: An alternative interpretation for the evolution of the southern margin of the North China Craton. *Lithos,* 102, p.158-178. DOI: 10.1016/j.lithos.2007.09.004

Herzberg, C., 1995. Generation of plume magmas through time: an experimental approach. *Chemical Geology,* 126, p.1-16. DOI: 10.1016/0009-2541(95)00099-4

Herzberg, C., Asimow, P.D., Arndt, N., Niu, Y., Lesher, C.M., Fitton, J.G., and Saunders, A.D., 2007. Temperature in ambient mantle and plumes: Constraints from basalts, picrites, and komatiites. *Geochemistry, Geophysics, Geosystems,* 8 (2). DOI: 10.1029/2006GC001390

Hollocher, K., Robinson, P., Walsh, E., and Roberts, D., 2012. Geochemistry of amphibolite-facies volcanics and gabbros of the Støren Nappe in extensions west and southwest of Trondheim, Western Gneiss Region, Norway: a key to correlations and paleotectonic settings. *American Journal of Science,* 312 (4). DOI: 10.2475/04.2012.01

Irvine, T.N. and Baragar, W.R.A., 1971, A guide to the chemical classification of the common volcanic rocks. *Canadian Journal of Earth Sciences,* 8 (5), p. 523-548. DOI: 10.1139/e71-055

Jafri, S.H. and Sheikh, J.M., 2013. Geochemistry of pillow basalts from Bompoka, Andaman-Nicobar Islands, Bay of Bengal, India. *Journal of Asian Earth Sciences,* 64, p.27-37. DOI: 10.1016/j.jseaes.2012.11.035

Jensen, L.S., 1976. A New Cation Plot for Classifying Subalkalic Volcanic Rocks.Ontario Division of Mines, MP 66, 22pp.

Kawachi, Y. and Pringle I.J., 1988.Multiple rind structure in pillow lava as an indicator of shallow water. *Bulletin of Volcanology,* 50, p.161-168. DOI: 10.1007/BF01079680

Kelemen, P.B., 1995. Genesis of high Mg# andesites and the continental crust.*Contributions to Mineralogy and Petrology,* 120, p.1-19. DOI: 10.1007/BF00311004

Kinzler, R.J., 1997. Melting of mantle peridotite at pressures approaching the spinel to garnet transition: Application to mid-ocean ridge basalt petrogenesis. *Journal of Geophysical Research,* 102, p.852-874. DOI: 10.1029/96JB00988.

Kersting, A.B. and Arculus, R.J., 1994. Klyuchevskoy Volcano, Kamchatka, Russia: The Role of High-Flux Recharged, Tapped, and Fractionated Magma Chamber(s) in the Genesis of High-Al_2O_3 from High-MgO Basalt. *Journal of Petrology,* 35 (1), p.1-41. DOI: 10.1093/petrology/35.1.1

Le Bas, M.J, Le Maitre, RW, Streckeisen, A, and Zanettin, B., 1986. A Chemical classification of volcanic rocks based on the total alkali-silica diagram. *Journal of Petrology,* 27, p.745-750. DOI: 10.1093/petrology/27.3.745

McDonough, W.F. and Sun, S.S., 1995. The composition of the Earth. *Chemical Geology,* 120, p.223-253.

MacLean, W.H., and Barrett, T.J., 1993. Lithogeochemical technique using immobile elements. *Journal of Geochemical Exploration,* 48 (2), p.109-133.

Nelson, Stephen A., 2011. *Igneous Rocks of the Convergent Margins*.https://www.tulane.edu/~sanelson/eens212/converg_margins.htm.

Middlemost, .E.A.K., 1975. The Basalt Clan. *Earth Science Reviewa,* 11(4), p.337-364. DOI:10.1016/0012-8252(75)90039-2.

Miyashiro, A., 1974. Volcanic rock series in island arcs and active continental margins. *American Journal of Science,* 274, p.321-355.

Mullen, E.D., 1983. MnO/TiO2/P2O5: a minor element discriminant for basaltic rocks of oceanic environments and its implications for petrogenesis. *Earth and Planetary Science Letters,* 62, p.53-62.

Nesbitt, H.W. and Wilson, R., 1992. Recent chemical weathering of basalts. *American Journal of Science,* 292, p.740-777.

Pearce, J.A., 1983. Role of subcontinental lithosphere in magma genesis at active continental margins. *In*: Hawkesworth, C.J., and Norry, M.J. (eds.), *Continental Basalt and Mantle Xenoliths*. Shiva Pub. Ltd., p.230-249.

Pearce, J.A. and Cann, J.R., 1973, Tectonic setting of basic volcanic rocks determined using trace element analyes. *Earth and Planetary Science Letters,* 19, p.290-300.

Pearce, T.H., Gorman, B.E., and Birkett, T.C., 1975. The TiO_2–K_2O–P_2O_5 diagram: A method of discriminating between oceanic and non-oceanic basalts. *Earth and Planetary Science Letters,* 24 (3), p.419-426.

Pearce, T.H., Gorman, B.E., and Birkett, T.C., 1977. The Relationship between Major Element Chemistry and Tectonic Environment of Basic and Intermediate Volcanic Rocks. *Earth and Planetary Science Letters,* 36, p.121-132. DOI: 10.1016/0012-821X (77)90193-5.

Pearce, J.A. and Norry, M.J., 1979. Petrogenetic implications of Ti, Zr, Y, and Nb. Variations in volcanic rocks*: Contributions to Mineralogy and Petrology,* 69*,* p.33-37.

Plank, T. and Langmuir, C.H., 1998. The chemical composition of subducting sediment and its consequence for the crust and mantle. *Chemical Geology,* 145, p.325-94.

Purwasatriya, E.B., Surjono, S.S., and Amijaya, D.H., 2017.Oligocene-Pleistocene Paleogeography within Banyumas Basin and Implication to Petroleum Potential. *Proceedings of 3rd International Conference on Science and Technology (ICST), UGM, Yogyakarta.*

Rudnick, R.L. and Gao, S., 2003. Composition of the Continental Crust. *In*: Holland, H.D. and Turekian, K.K., 2010 (eds.), *Readings from the Treatise on Geochemistry* (1st Edition). p.131-195.

Salters, V.J.M. and Stracke, A., 2004. Composition of the depleted mantle. *Geochemistry, Geophysics, Geosystems,* 5 (5). DOI: 10.1029/2003GC000597.

Schilling, J.G., Zajac, M., Evans. R., Johnston. T., White. W., Devine, J. D., and Kingsley, R., 1983. Petrologic and geochemical variations along the Mid-Atlantic Ridge from 27°N to 73°N. *American Journal of Science,* 283, p.510-86.

Sendjaja, Y.A., Kimura, J.I., and Sunardi, E., 2009. Across-arc geochemical variation of Quaternary lavas in West Java, Indonesia: Mass-balance elucidation using arc basalt simulator model. *Island Arc,* 18, p.201-224.

Streckeisen, A. L., 1978. IUGS Subcommission on the Systematics of Igneous Rocks. Classification and Nomenclature of Volcanic Rocks, Lamprophyres, Carbonatites and Melilite Rocks.Recommendations and Suggestions.*Neues Jahrbuch für Mineralogie, Abhandlungen,* 141, p.1-14.

Schnur, S.R., 2007. An Analysis of the Morphology and Physical Properties of Pillow Lavas of the Nicasio Reservoir Terrane, Marin County, California: Implications for Seamount Formation and Structure. Senior Integrative Exercise, Submitted in partial fulfillment of the requirements for a Bachelor of Arts degree from Carleton College, Northfield, Minnesota.

Talbi, E.H. and Honnorez, J., 2003. Low-temperature Alteration of Mesozoic Oceanic Crust, Ocean Drilling Program Leg 1855. *Journal of Geochemistry Geophysic Geosystem.* 4 (8906), DOI:10.1029/2002GC000405.

Taylor, S.R. and McLennan, S.M., 1985. *The Continental Crust: Its Composition and Evolution*. Blackwell, Oxford. 312pp.

Turner, S. and Foden, J., 2001. U, Th and Ra disequilibria, Sr, Nd, and Pb isotope and trace element variations in Sunda arc lavas: Predominance of a subducted sediment component.*Contributions to Mineralogy and Petrology,* 142, p.43-57.

Whitney, D.L. and Evans, B.W., 2010. Abbreviations for names of rock-forming minerals. *Journal of American Mineralogist,* 95, p.185-187.

Wilson, M., 1989. *Igneous Petrogenesis - A Global Tectonic Approach.* Published by Harper Collins Academic, London, UK, 466 pp.

Zulkarnain, I., 2011. Geochemical Evidence of Island-Arc Origin for Sumatra Island; A New Perspective based on Volcanic Rocks in Lampung Province, Indonesia. *Jurnal Geologi Indonesia,* 6 (4)*,* p.213-225.

Zhang, Y.X., 2014. Quantification of the elemental incompatibility sequence, and composition of the "superchondritic" mantle. *Chemical Geology,* 369, p.12-21